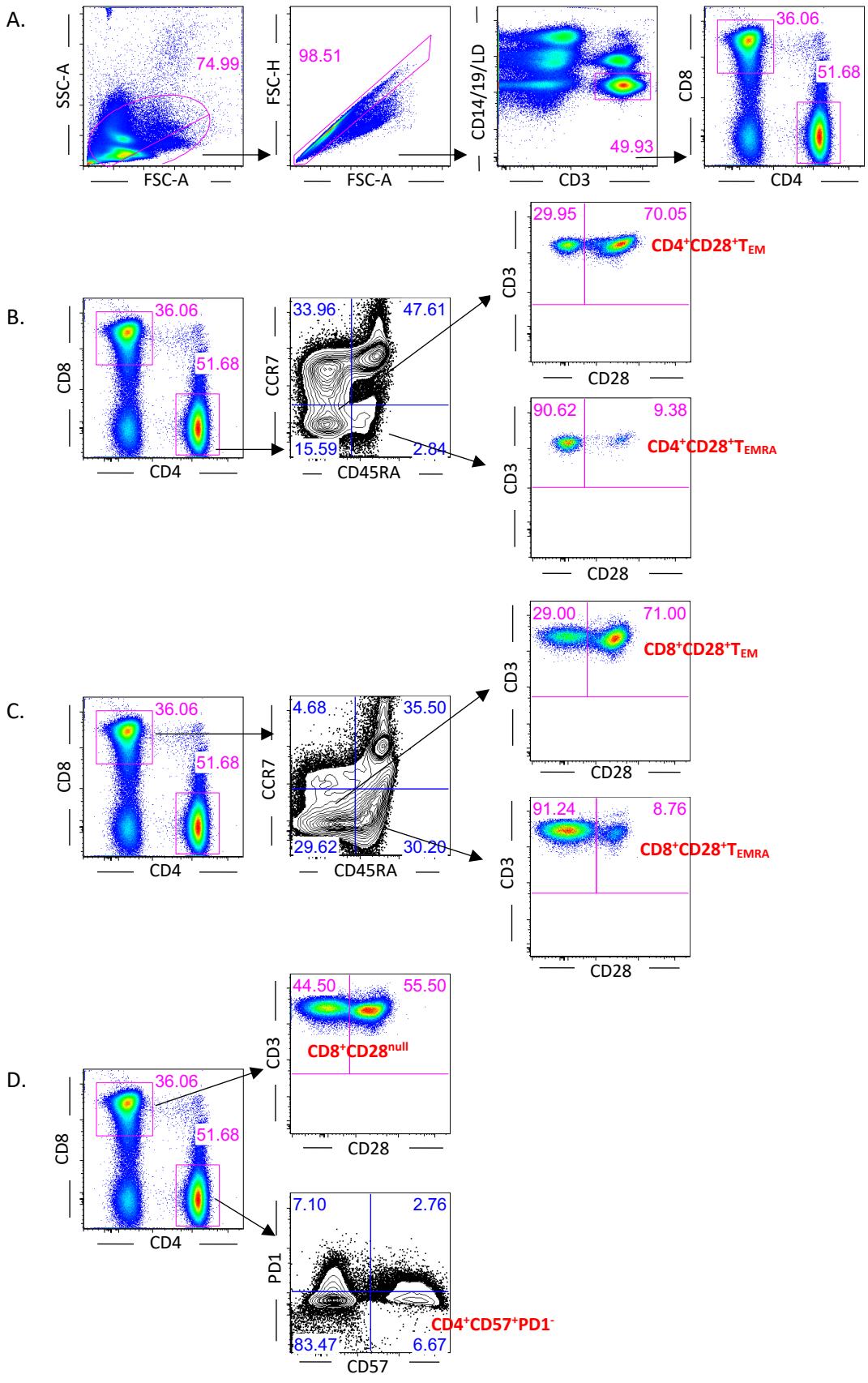

Supplemental Figure 1. Gating strategy to identify "risky" memory T cell subsets associated with belatacept-resistant rejection. Representative flow plots of the gating strategy to identify (A) $CD4^+$ and $CD8^+$ T cells, (B) $CD4^+$ $CD28^+$ T_{EM} and $CD4^+$ $CD28^+$ T_{EMRA} subsets, (C) $CD8^+$ $CD28^+$ T_{EM} and $CD8^+$ $CD28^+$ T_{EMRA} subsets, (D) $CD8^+$ $CD28^{null}$ and $CD4^+$ $CD57^+$ $PD1^-$ subsets.

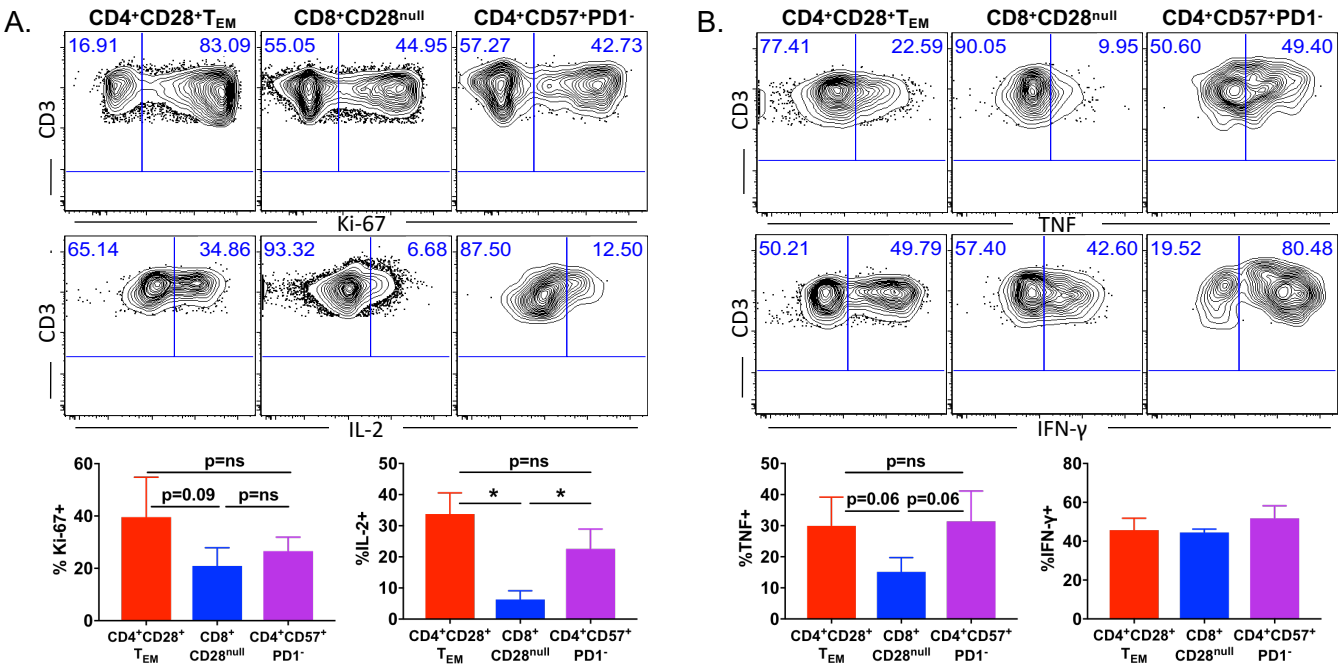

Supplemental Figure 2. Characterization of "risky" memory T cell subsets associated with belatacept-resistant rejection. Human PBMCs from healthy donors were stimulated ex vivo with anti-CD3/CD28 beads for 3 d followed by brief restimulation in the presence or absence of PMA/Iono. Risky memory T cell subsets were defined as in Figure 1. (A) Representative flow plots and summary data of frequencies of Ki-67$^+$ proliferating cells and IL-2-secreting cells within risky memory T cell subsets after stimulation. (B) Representative flow plots and summary data of frequencies of TNF-producing cells and IFN-γ-producing cells within risky memory T cell subsets after stimulation (*, $p < 0.05$; n = 6 per experiment; data are representative of three independent experiments).

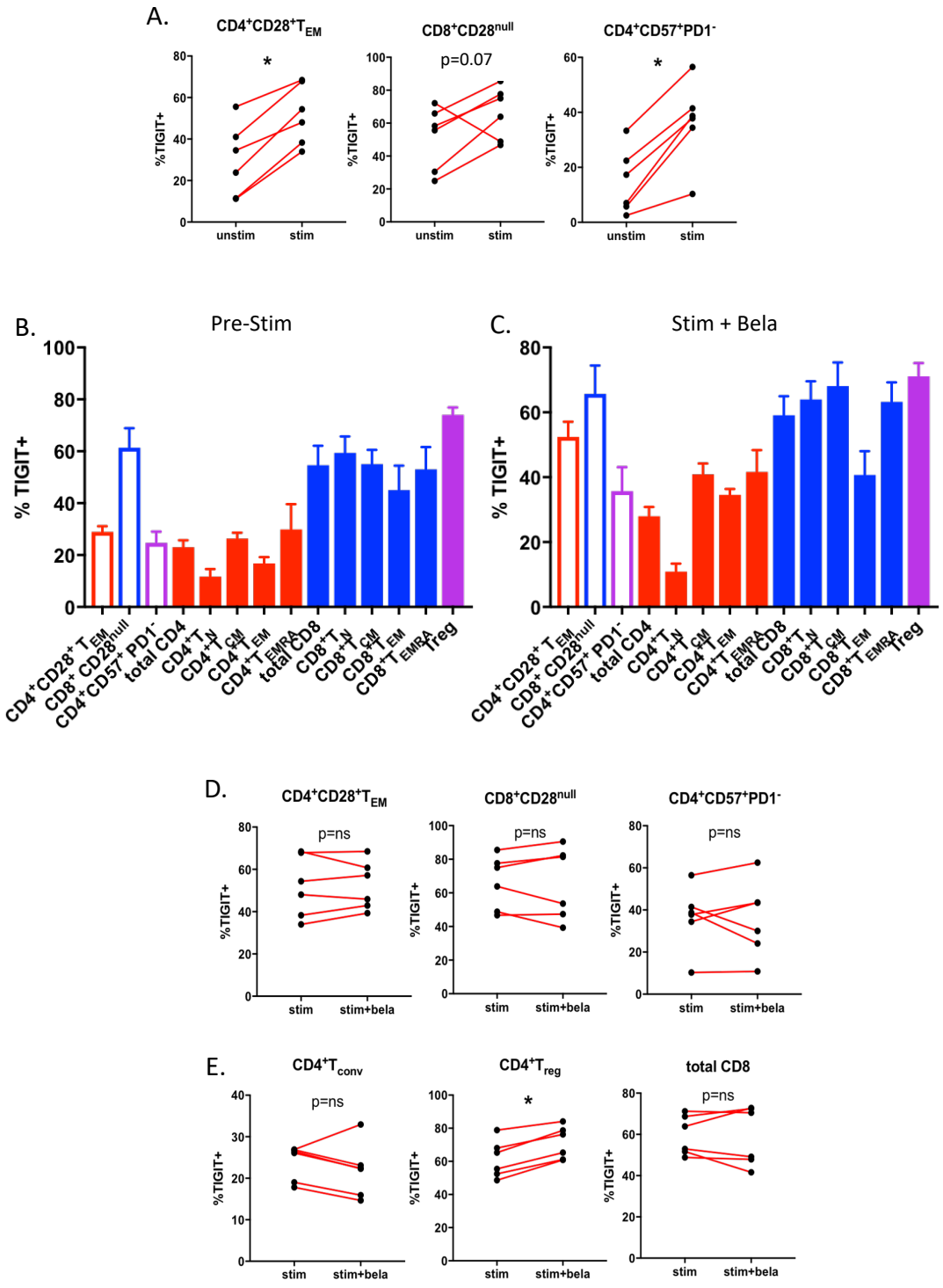

Supplemental Figure 3. TIGIT expression is increased following ex vivo restimulation but not further increased by exposure to belatacept. Peripheral blood T cells from healthy donors were left unstimulated or were stimulated ex vivo using anti-CD3/CD28 beads in the presence or absence of belatacept. TIGIT expression on the different memory T cell subsets in the various conditions is shown (*, $p < 0.05$; n = 6 per experiment; data are representative of three independent experiments).

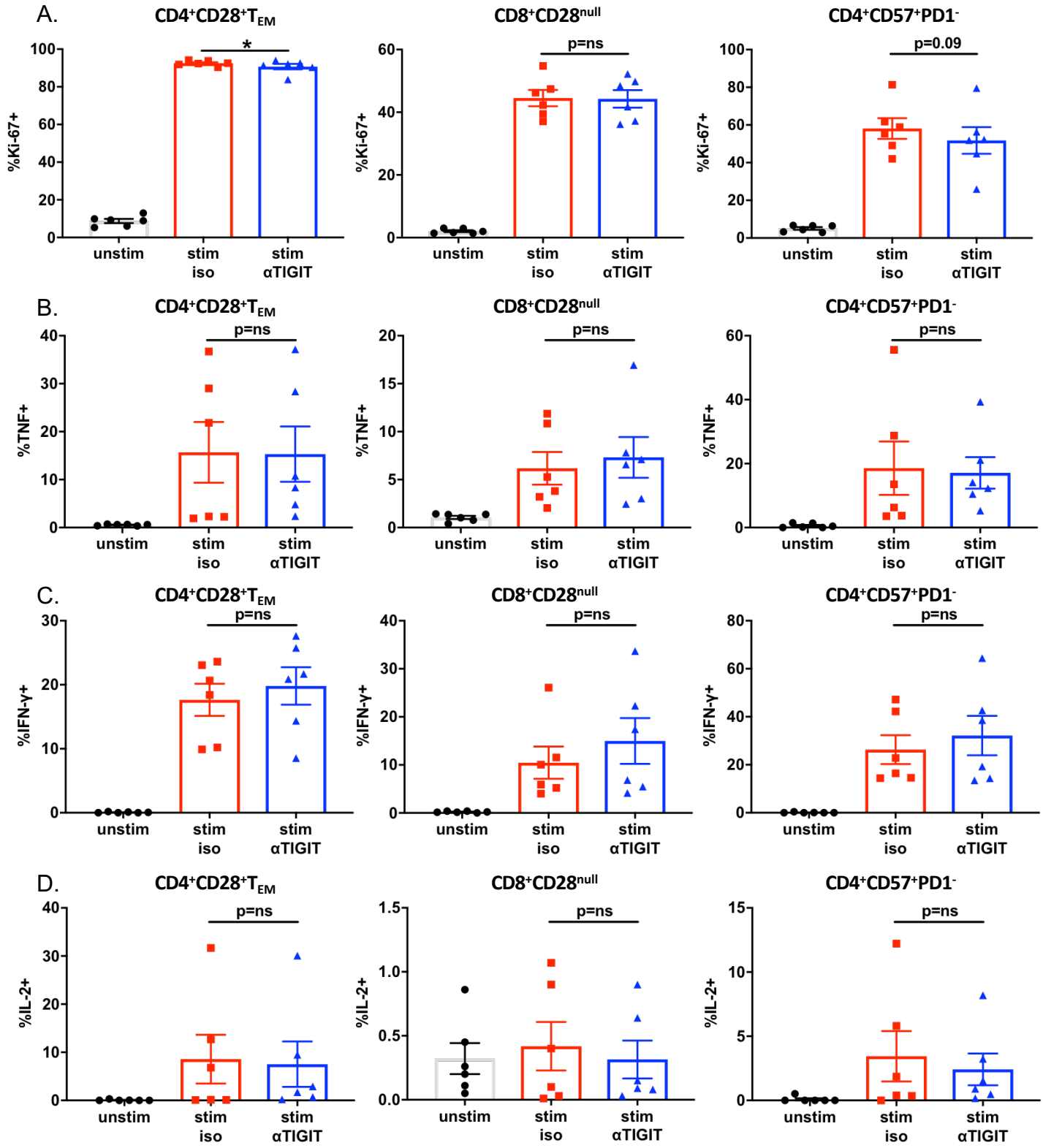

Supplemental Figure 4. Agonistic αTIGIT does not differentially affect the proliferation and cytokine effector function of "risky" memory T cell subsets. Peripheral blood T cells from healthy donors were left unstimulated or were stimulated ex vivo in the presence of agonistic αTIGIT or isotype control. Risky memory T cell subsets were defined as in Figure 1. Summary data of frequencies of Ki-67^{+} proliferating cells (A), TNF-secreting cells (B), IFN-γ-secreting cells (C) and IL-2-secreting cells (D) within risky memory T cell subsets (*, $p < 0.05$; n = 6 per experiment; data are representative of three independent experiments).

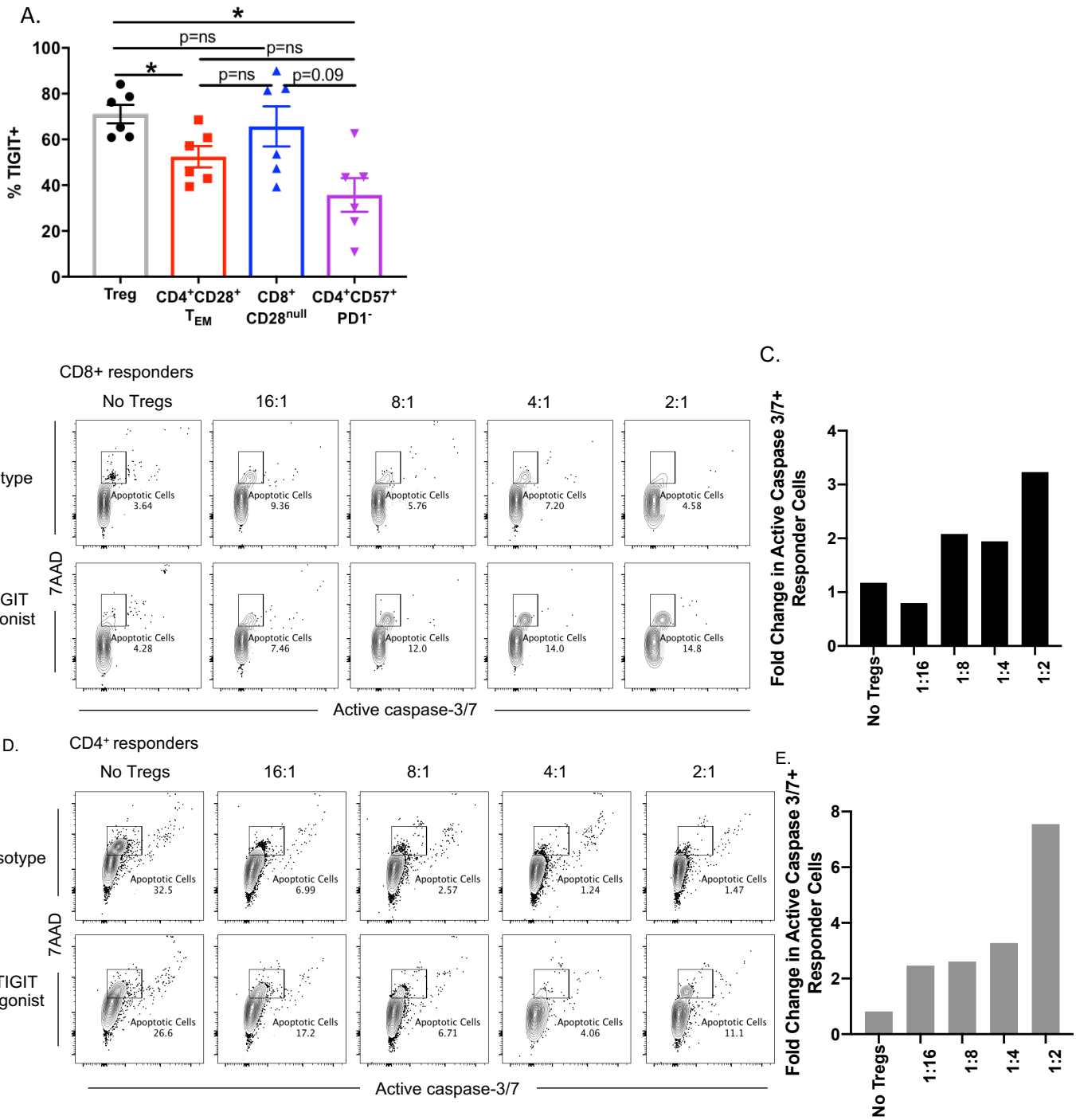

Supplemental Figure 5. TIGIT agonism induces apoptosis of CD4⁺ and CD8⁺ T cells in a Treg-dependent manner. A, Frequencies of TIGIT⁺ cells among FOXP3⁺ Treg and memory T cell subsets. B, Human Tregs were purified from PBMC using CD4⁺ negative selection followed by CD25⁺ positive selection and were cultured in the presence of increasing numbers of conventional CD8⁺ (B, C) or CD4⁺ (D, E) T cells in presence of either the agonistic anti-TIGIT antibody or an isotype control. Cultures were stimulated with anti-CD3/anti-CD28 DynaBeads, and active caspase-3/7⁺ cells were enumerated via flow cytometry at d5. The fold change in caspase3/7⁺ in T cells from TIGIT agonist-treated cultures vs. isotype-treated wells is depicted (C, E).